

No-reference Synthetic Image Quality Assessment using Scene Statistics

Debarati Kundu and Brian L. Evans
Embedded Signal Processing Laboratory
The University of Texas at Austin, Austin, TX
Email: debarati@utexas.edu, bevans@ece.utexas.edu

Abstract—Measuring visual quality, as perceived by human observers, is becoming increasingly important in many applications where humans are the ultimate consumers of visual information. Significant progress has been made for assessing the subjective quality of natural images, such as those taken by optical cameras. Natural Scene Statistics (NSS) is an important tool for no-reference visual quality assessment of natural images, where the reference image is not needed for comparison. In this paper, we take an important step towards using NSS to automate visual quality assessment of photorealistic synthetic scenes typically found in video games and animated movies. Our primary contributions are (1) conducting subjective tests on our publicly available ESPL Synthetic Image Database containing 500 distorted images (20 distorted images for each of the 25 original images) in 1920×1080 format, and (2) evaluating the performance of 17 no-reference image quality assessment (IQA) algorithms using synthetic scene statistics. We find that similar to natural scenes, synthetic scene statistics can be successfully used for IQA and certain statistical features are good for certain image distortions.

I. INTRODUCTION

Recently there has been an immense growth in acquisition, transmission and storage of video data, which consists of synthetic scenes (such as animated movies, cartoons and video games) in addition to the natural videos captured with optical cameras. In all these cases, methods of evaluating the visual quality provide important tools for the optimal design of displays, rendering engines and maintaining a satisfactory quality-of-experience in video streaming applications under certain bandwidth constraints.

For full-reference image quality assessment (IQA) metrics, the distortions in an image are compared to a reference “pristine” image. However, for applications where the ground-truth reference image is not available, blind or no-reference IQA (NR-IQA) metrics are better suited. Most of the NR metrics are based on learning based approaches using statistical properties possessed by pristine images, which for natural images tend to appear irrespective of image content and it is assumed that distortions tend to deviate the Natural Scene Statistics (NSS). Some of the popular NR-IQA metrics for natural images described in [1] [2] [3] [4].

However, these metrics for evaluating the quality of natural images have not been studied in the context

of images generated using computer graphics. With the improvement of graphics engines, synthetic images are becoming increasingly photo-realistic, which has made us to conjecture that with some modifications, the NSS based NR-IQA metrics can be potentially applied to computer graphics. In our earlier work [5], we modeled the distribution of mean-subtracted-contrast-normalized (MSCN) pixels obtained from the synthetic image intensities using Generalized Gaussian and Symmetric α -Stable distributions similar to natural images.

Recently we conducted a subjective test on 64 observers, each of whom evaluated more than 500 photo-realistic synthetic images (pristine and distorted images) [6] and compiled the results for our ESPL Synthetic Image Database [7]. Some of the most popular natural image databases are LIVE Image Quality Database (LIVE) [8], Tampere Image Database 2013 [9], Categorical Image Quality Database [10] and EPFL JPEG XR codec [11]. Recently Čadík *et al.* have developed a database of computer graphics generated imagery [12].

From our ESPL Synthetic Image Database, we consider a larger number of photo-realistic images and a broader class of distortions (transmission and compression artifacts for synthetic images) than the work by Čadík *et al.* [12] [13] in the hope of providing a better representation of the types of images and artifacts encountered in watching animated movies and playing video games. In this paper, we use benchmark the state-of-the-art NR-IQA metrics on our database.

Čadík *et al.* [13] proposes an NR-IQA metric for quantifying rendering distortions based on machine learning. The features were chosen heuristically, instead of analyzing the properties of the synthetic images under test.

In this paper, we (1) conduct subjective tests on our publicly available ESPL Synthetic Image Database, and (2) compare 17 no-reference IQA algorithms to the subjective test results. The comparison includes hypothesis testing and statistical significance analysis. We evaluate the applicability of NSS in different domains to synthetic scenes and observe how the presence of distortions change the scene statistics for synthetic images.



Fig. 1: Sample synthetic images in the ESPL database [6]

II. USE OF THE ESPL DATABASE

For the purpose of this study, 25 synthetic images have been chosen from video games and animated movies. These high quality color images from the Internet are 1920×1080 pixels in size. Three categories of processing artifacts have been considered, namely interpolation (which arises frequently in texture maps, causing jaggedness of crisp edges), blurring (“Blur”) and additive Gaussian noise (“GN”). With the advent of cloud gaming, where the rendered 2D game images are streamed from the server to the ‘dumb’ clients, we have chosen to study the effect of compression and transmission artifacts on computer graphics generated images (which had been previously considered only for natural scenes). For this database, JPEG compression (“JPEG”) and Rayleigh fast-fading wireless channel artifacts (“FF”) have been considered. For each artifact type, four different levels were considered, resulting in 20 distorted image created from a single pristine image.

A single stimulus continuous evaluation testing procedure [14] was followed. 64 subjects evaluated each image on a Dell 24 inches U2412M display. 12 subjects were treated as outliers and the ratings obtained from the remaining 52 subjects were considered in the calculation of the final differential mean opinion score (DMOS) for each image. Details on the type of artifacts and the testing methodology can be found in [7].

III. EXPERIMENTAL RESULTS

A. NSS on Synthetic Scenes

Leading NR-IQAs are based on the premise that natural images occupy a small subspace of all possible two dimensional signals, and that distortions deviate from NSS (Fig. 2). In this study we find that similar conclusions about distortions also hold for synthetic images. Different NR-IQAs use NSS in either in the spatial domain or in transform domains, such as using DCT, Gabor or wavelet domains.

1) *Spatial Domain Features*: In [15], it was observed that for natural images MSCN pixels tend to follow a Gaussian-like distribution. Distribution of MSCN pixels along with those of their paired products has been employed in Blind/Referenceless Image Spatial

QUALity Evaluator (BRISQUE) [3] and Natural Image Quality Evaluator (NIQE) [16]. The Derivative Statistics-based QUALity Evaluator (DESIQUE) [4] supplements BRISQUE by using log-derivative distributions of MSCN pixels. In a gradient magnitude (GM) map and the Laplacian of Gaussian (LOG) response based NR-IQA metric (GM-LOG) [17], the GM has been computed after applying Gaussian partial derivative filters along the horizontal and vertical directions. This along with LOG response, captures the Luminance discontinuities.

2) *Transform Domain Features*: Neurons employed in early stages of the visual pathway capture information over multiple orientation and scales, which has led to multiscale processing in many NR-IQAs: log-Gabor decomposition (DESIQUE [4]), steerable pyramid wavelets (Distortion Identification-based Image Verity and INTEGRity Evaluation - DIIVINE [1]), Daubechies 9/7 wavelets (Blind Image Quality Index - BIQI [18]), DCT (BLind Image Integrity Notator using DCT Statistics-II - BLIINDS-II [2]), phase congruency (General Regression Neural Network IQA - GRNN [19]), curvelets (CurveletQA [20]), expected image entropy upon a set of predefined directions (Anisotropy [21]). In contrary, CODEbook Representation for No-Reference Image Assessment (CORNIA) [22] uses supervised learning technique to learn a dictionary for different distortions from the raw image patches instead of using a fixed set of features.

B. NSS of distorted images

As in the case of natural images, for synthetic images also we find that the presence of distortions change the scene statistics based features extracted from the image patches. For three NR-IQA algorithms, Fig. 3 shows the features for each distortion class projected onto a two-dimensional space using Principle Component Analysis. Pristine images and images with different types of distortions form different clusters, which show that the NSS based features can be used for distortion classification. Table I shows the distortion classification accuracy of

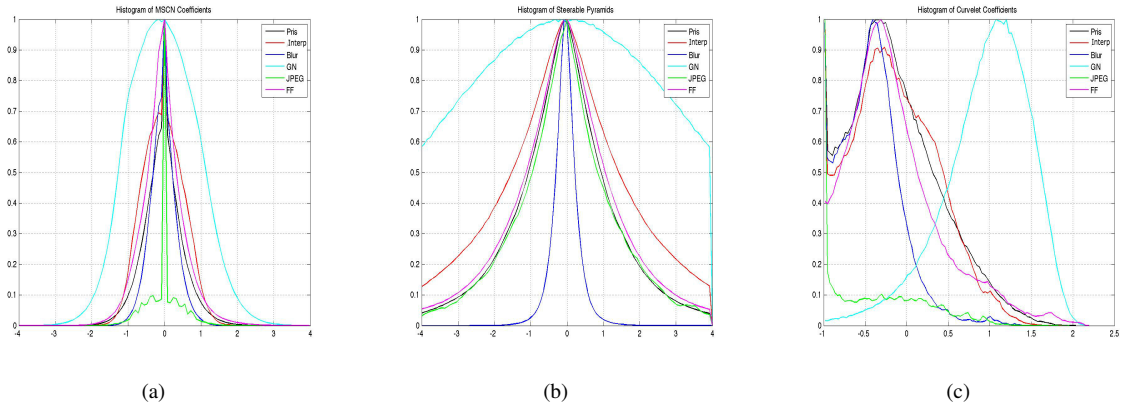


Fig. 2: Histograms of (a) MSCN pixels, (b) Steerable Pyramid Wavelet Coefficients and (c) Curvelet Coefficients of pristine and distorted image patches obtained from ESPL Synthetic Image Database. The figure shows how distortions change the statistics of pristine images.¹

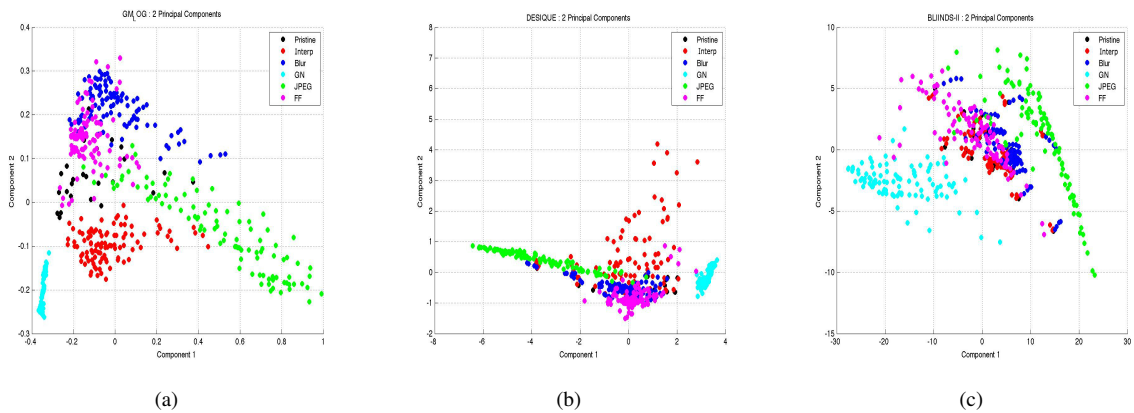


Fig. 3: Features used in (a) GM-LOG (b) DESIQUE (c) BLINDS-II NR-IQAs projected onto 2 dimensional space using Principal Component Analysis. Pristine images and images with different types of distortions (obtained from the ESPL Synthetic Image Database) form different clusters.¹

the features used in popular NR-IQA algorithms.

IQA	Interpolation	Blur	GN	JPEG	FF	All
GM-LOG	100.0	96.0	100.0	96.5	96.6	97.8
BRISQUE	94.4	96.6	100.0	91.8	89.8	94.4
DESIQUE	92.5	88.5	100.0	87.9	88.2	91.4
BIQI	88.8	92.3	93.8	93.8	88.0	91.2
BLINDS-II	91.6	87.7	100.0	82.0	82.7	88.7
CurveletQA	88.4	85.8	100.0	81.3	74.6	85.9
DIIVINE	46.1	75.9	79.1	58.3	49.9	61.5

TABLE I: Mean classification accuracy (in percentage) for various Image Quality Assessment (IQA) algorithms across 100 train-test (4:1) combinations on ESPL database.

C. Performance of NR-IQA algorithms

In the paper, on the ESPL Synthetic Image Database, we have evaluated the performance of 11 distortion

¹Legends Pris, Interp, Blur, GN, JPEG, FF refer to pristine images, images with interpolation distortion, blur distortion, additive white Gaussian noise, compressed with JPEG encoder and transmitted over a Rayleigh fast-fading wireless channel, respectively.

agnostic NR-IQA algorithms (DESIQUE [4], GM-LOG [17], BRISQUE [3], CORNIA [22], BLINDS-II [2], CurveletQA [20], DIIVINE [1], BIQI [18], GRNN [19], NIQE [16] and Anisotropy [21]), 5 NR-IQA algorithms (LPCM [23], CPBDM [24], FISH [25], S_3 [26] and JNBM [27]) for blurred and one NR-IQA algorithm (JPEG-NR [28]) for JPEG compressed images. The performances of full-reference IQA (FR-IQA) algorithms like Peak Signal-to-noise Ratio (PSNR) and Multi-scale Structural Similarity Index (MS-SSIM) have also been provided for reference.

For rows 1-8, after the feature extraction step, a mapping is obtained from the feature space to the DMOS scores using a regression method, which provides a measure of the perceptual quality. We used a support vector machine regressor (SVR), LibSVM software [29] is used to implement ϵ -SVR with radial basis function kernel. Image of the ESPL database were split randomly into two subsets (80% training and 20% testing) and the process was repeated 100 times to eliminate any bias due

No.	IQA	Interpolation		Blur		GN		JPEG		FF		All		Runtime (seconds)
		SROCC	PLCC											
1	DESIQUE	0.7495	0.7865	0.8834	0.8947	0.9242	0.9601	0.9461	0.9691	0.8126	0.8557	0.8872	0.8817	1.78
2	GM-LOG	0.8328	0.8486	0.8211	0.8441	0.8793	0.9409	0.9076	0.9374	0.7945	0.8242	0.8678	0.8536	0.51
3	BRISQUE	0.6699	0.6899	0.8105	0.8388	0.8714	0.9267	0.9261	0.9403	0.7737	0.7996	0.8554	0.8382	0.53
4	CORNIA	0.8000	0.8395	0.8701	0.8929	0.8584	0.8812	0.8844	0.9255	0.7774	0.8064	0.8471	0.8478	84.33
5	BLIINDS-II	0.8003	0.8313	0.8559	0.8744	0.9024	0.9240	0.8947	0.9169	0.7930	0.8493	0.8379	0.8492	74.50
6	CurveletQA	0.7720	0.7992	0.7796	0.8472	0.8973	0.9516	0.9022	0.9177	0.6798	0.7235	0.7998	0.8081	16.29
7	DIIVINE	0.7434	0.7695	0.8007	0.8201	0.8116	0.8542	0.7750	0.8149	0.5497	0.5412	0.7547	0.7143	118.31
8	BIQI	0.7264	0.7627	0.8443	0.8672	0.9071	0.9493	0.8075	0.8290	0.5889	0.6565	0.7513	0.7061	1.95
9	MS-SSIM	0.6230	0.6347	0.6457	0.6498	0.9082	0.9237	0.8710	0.8907	0.9029	0.9005	0.6994	0.7121	0.90
10	PSNR	0.5651	0.5908	0.4811	0.4920	0.8638	0.8973	0.6952	0.7016	0.8456	0.8585	0.5903	0.6030	0.02
11	GRNN	0.5568	0.5875	0.6022	0.6451	0.8502	0.9232	0.7573	0.7812	0.6177	0.6503	0.5415	0.5225	3.41
12	NIQE	0.3643	0.3539	0.3565	0.3999	0.8351	0.8708	0.3846	0.4485	0.3921	0.4391	0.4697	0.4306	2.30
13	Anisotropy	0.3670	0.3758	0.4373	0.3530	0.7411	0.6806	0.1593	0.2267	0.4111	0.4688	0.2196	0.3113	10.13
14	LPCM	<i>0.4155</i>	<i>0.4436</i>	0.8358	0.8470	<i>0.6227</i>	<i>0.6213</i>	<i>0.2111</i>	<i>0.2311</i>	<i>0.1079</i>	<i>0.2367</i>	-	-	0.86
15	CPBDM	<i>0.6761</i>	<i>0.7200</i>	0.7568	0.7664	<i>0.7457</i>	<i>0.8151</i>	<i>0.7646</i>	<i>0.7489</i>	<i>0.3474</i>	<i>0.4045</i>	-	-	0.95
16	FISH	<i>0.2222</i>	<i>0.3051</i>	0.7045	0.7159	<i>0.8226</i>	<i>0.8696</i>	<i>0.1961</i>	<i>0.2519</i>	<i>0.4322</i>	<i>0.4716</i>	-	-	0.47
17	S_3	<i>0.4086</i>	<i>0.4493</i>	0.7001	0.7558	<i>0.7468</i>	<i>0.7859</i>	<i>0.1509</i>	<i>0.1889</i>	<i>0.4024</i>	<i>0.4503</i>	-	-	276.20
18	JNBM	<i>0.5979</i>	<i>0.6347</i>	0.5063	0.5283	<i>0.7556</i>	<i>0.8155</i>	<i>0.5355</i>	<i>0.5121</i>	<i>0.4482</i>	<i>0.4551</i>	-	-	0.41
19	JPEG-NR	<i>0.5403</i>	<i>0.5703</i>	<i>0.5929</i>	<i>0.6501</i>	<i>0.7483</i>	<i>0.8648</i>	<i>0.9277</i>	<i>0.9540</i>	<i>0.4643</i>	<i>0.6068</i>	-	-	0.71

TABLE II: Median Spearman’s Rank Ordered Correlation Coefficient (SROCC) and Pearson’s Linear Correlation Coefficient (PLCC) between algorithm scores and DMOS for various Image Quality Assessment (IQA) algorithms (described in Section III-C) along with the time needed (on a Macintosh laptop having 8 GB RAM, 2.9 GHz clock, Intel Core i7 CPU) across 100 train-test (4:1) combinations on the ESPL Synthetic Image Database. Italicized IQA algorithms are full-reference algorithms. Italicized correlations indicate the values obtained when the mentioned NR-IQA algorithms were applied for distortion categories other than what they were originally intended for.

	PSNR	MS-SSIM	DESIQUE	BRISQUE	BLIINDS-II	DIIVINE	BIQI	CurveletQA	GM-LOG	GRNN
PSNR	-----	-----	---010	---010	---0-0	0---1-	00--1-	0--010	---0-0	----1-
MS-SSIM	-----	-----	---0-0	---0-0	---0-0	0-----	00-----	0-----0	0--0-0	-----
DESIQUE	---101	---1-1	-----	-----	-----	---1-1	---1-1	---1--	-----	-1-1-1
BRISQUE	---101	---1-1	-----	-----	-----	---1-1	---1-1	-----	-----	-1-1-1
BLIINDS-II	---1-1	---1-1	-----	-----	-----	---1--	---1-1	-----	-----	-1-1-1
DIIVINE	1---0-	1-----	---0-0	---0-0	---0--	-----	-0-----	-----	---0-0	-----
BIQI	11--0-	11-----	---0-0	---0-0	---0-0	-1-----	-----	---0--	---0-0	-1-----
CurveletQA	1--101	1----1	---0--	-----	-----	-----	---1--	-----	-----	-11--1
GM-LOG	---1-1	1--1-1	-----	-----	-----	---1-1	---1-1	-----	-----	-1-1-1
GRNN	----0-	-----	-0-0-0	-0-0-0	-0-0-0	-----	-0-----	-00--0	-0-0-0	-----

TABLE III: Results of the F-test performed on the residuals between model predictions and DMOS values. In each cell, the symbol of 6 entries indicates ‘Interpolation’, ‘Blur’, ‘GN’, ‘JPEG’, ‘FF’ and ‘All’ respectively.

to varying spatial content.

From Tables I and II we find that DESIQUE, BRISQUE and GM-LOG features are best performing in both the tasks of distortion classification and deducing the mapping between the feature space and the DMOS scores. All of the SVM based NR-IQA algorithms beat FR-IQA algorithms like PSNR and MS-SSIM. GRNN, NIQE and Anisotropy do worse than FR-IQA algorithms. NIQE, which does remarkably well for natural images performs poorly on being trained on pristine synthetic images. This might occur due to higher amount of variability in the distribution of the MSCN coefficients for synthetic images as compared to natural scenes [5]. Compared to IQA algorithms meant for particular distortion classes (rows 14-19), scene statistics based algorithms (rows 1-8) perform better. The NR-IQA algorithms perform worse on the ‘Interpolation’ artifact. This is because low down-sampling factors result in near-threshold artifacts, which might appear almost imperceptible, specially at normal viewing distances.

To determine whether the IQA algorithms are significantly different from each other, the F-statistic, as in [8] [30], was used to determine the statistical significance between the variances of the residuals after a non-linear logistic mapping between two IQA algorithms. Table III shows the results for eight selected NR-IQA algorithms and two full-reference IQA algorithms across all distortions. The value of ‘1’ (‘0’) indicates that the row IQA is statistically better (worse) than the column IQA, ‘-’ implies statistical equivalence of the row and the column. Some of the best performing NR-IQA algorithms, such as DESIQUE, BRISQUE, BLIINDS-II, GM-LOG, CurveletQA etc are found to be statistically superior to PSNR and MS-SSIM.

IV. CONCLUSION

In this paper we have studied the successful applicability of scene statistics approach to synthetic images in our ESPL Synthetic Image Database and benchmarked 17 state-of-the-art publicly available NR-IQA algorithms.

REFERENCES

- [1] A. K. Moorthy and A. C. Bovik, "Blind image quality assessment: From natural scene statistics to perceptual quality," *IEEE Transactions on Image Processing*, vol. 20, no. 12, pp. 3350–3364, Dec 2011.
- [2] M. A. Saad, A. C. Bovik, and C. Charrier, "Blind image quality assessment: A natural scene statistics approach in the DCT domain," *IEEE Transactions on Image Processing*, vol. 21, no. 8, pp. 3339–3352, 2012.
- [3] A. Mittal, A. K. Moorthy, and A. C. Bovik, "No-reference image quality assessment in the spatial domain," *IEEE Transactions on Image Processing*, vol. 21, no. 12, pp. 4695–4708, Dec 2012.
- [4] Y. Zhang and D. M. Chandler, "No-reference image quality assessment based on log-derivative statistics of natural scenes," *Journal of Electronic Imaging*, vol. 22, no. 4, 2013.
- [5] D. Kundu and B. L. Evans, "Spatial domain synthetic scene statistics," in *Proc. Asilomar Conference on Signals, Systems and Computers*, Nov 2014.
- [6] D. Kundu and B. L. Evans, "ESPL Synthetic Image Database Release 2," January 2015, <http://signal.ece.utexas.edu/~bevans/synthetic/>.
- [7] D. Kundu and B. L. Evans, "Full-reference visual quality assessment for synthetic images: A subjective study," in *Proc. IEEE Int. Conf. on Image Processing, Sep. 2015, accepted.*, September 2015, <http://users.ece.utexas.edu/~bevans/papers/2015/imagequality/index.html>.
- [8] H. R. Sheikh, M. F. Sabir, and A. C. Bovik, "A statistical evaluation of recent full reference image quality assessment algorithms," *IEEE Transactions on Image Processing*, vol. 15, no. 11, pp. 3440–3451, Nov 2006.
- [9] N. N. Ponomarenko, O. Jeremeiev, V. V. Lukin, L. Jin, K. Egiazarian, J. Astola, B. Vozel, K. Chehdi, M. Carli, F. Battisti, and C.-C. J. Kuo, "A new color image database TID2013: Innovations and results," in *Advanced Concepts for Intelligent Vision Systems*, ser. Lecture Notes in Computer Science. Springer International Publishing, 2013, vol. 8192, pp. 402–413.
- [10] E. C. Larson and D. M. Chandler, "Most apparent distortion: full-reference image quality assessment and the role of strategy," *Journal of Electronic Imaging*, vol. 19, no. 1, p. 011006, 2010.
- [11] F. De Simone, L. Goldmann, V. Baroncini, and T. Ebrahimi, "Subjective evaluation of JPEG XR image compression," in *Proceedings of SPIE*, vol. 7443, 2009.
- [12] M. Čadík, R. Herzog, R. Mantiuk, K. Myszkowski, and H.-P. Seidel, "New measurements reveal weaknesses of image quality metrics in evaluating graphics artifacts," *ACM Transactions on Graphics*, vol. 31, no. 6, pp. 147:1–147:10, Nov. 2012.
- [13] R. Herzog, M. Čadík, T. O. Aydın, K. I. Kim, K. Myszkowski, and H.-P. Seidel, "NoRM: No-Reference image quality metric for realistic image synthesis," *Computer Graphics Forum*, vol. 31, no. 2, pp. 545–554, 2012.
- [14] ITU-r BT.500-12 methodology for the subjective assessment of the quality of television pictures - IHS, inc. [Online]. Available: http://www.dii.unisi.it/~menegaz/DoctoralSchool2004/papers/ITU-R_BT.500-11.pdf
- [15] D. L. Ruderman and W. Bialek, "Statistics of natural images: Scaling in the woods," in *Neural Information Processing Systems Conference and Workshops*, 1993, pp. 551–558.
- [16] A. Mittal, R. Soundararajan, and A. C. Bovik, "Making a "completely blind" image quality analyzer," *IEEE Signal Processing Letters*, vol. 20, no. 3, pp. 209–212, 2013.
- [17] W. Xue, X. Mou, L. Zhang, A. C. Bovik, and X. Feng, "Blind image quality assessment using joint statistics of gradient magnitude and laplacian features," *IEEE Transactions on Image Processing*, vol. 23, no. 11, pp. 4850–4862, Nov 2014.
- [18] A. K. Moorthy and A. C. Bovik, "A two-step framework for constructing blind image quality indices," *IEEE Signal Processing Letters*, vol. 7, no. 5, May 2010.
- [19] C. Li, A. C. Bovik, and X. Wu, "Blind image quality assessment using a general regression neural network," *IEEE Transactions on Neural Networks*, vol. 22, no. 5, pp. 793–799, May 2011.
- [20] L. Liu, H. Dong, H. Huang, and A. C. Bovik, "No-reference image quality assessment in curvelet domain," *Signal Processing: Image Communication*, vol. 29, no. 4, April 2014.
- [21] S. Gabarda and G. Cristbal, "Blind image quality assessment through anisotropy," *Journal of the Optical Society of America*, vol. 24, no. 12, December 2007.
- [22] Peng Ye, Jayant Kumar, Le Kang, and David Doermann, "Un-supervised Feature Learning Framework for No-reference Image Quality Assessment," in *Proc. Intl. Conf. on Computer Vision and Pattern Recognition*, June 2012, pp. 1098–1105.
- [23] R. Hassen, Z. Wang, and M. Salam, "Image sharpness assessment based on local phase coherence," *IEEE Transactions on Image Processing*, vol. 22, no. 7, pp. 2798–2810, July 2013.
- [24] N. D. Narvekar and L. J. Karam, "A no-reference perceptual image sharpness metric based on a cumulative probability of blur detection," in *Proc. International Workshop on Quality of Multimedia Experience*, July 2009, pp. 87–91.
- [25] P. Vu and D. Chandler, "A fast wavelet-based algorithm for global and local image sharpness estimation," *IEEE Signal Processing Letters*, vol. 19, no. 7, pp. 423–426, July 2012.
- [26] C. T. Vu, T. Phan, and D. M. Chandler, " S_3 : A spectral and spatial measure of local perceived sharpness in natural images," *IEEE Transactions on Image Processing*, vol. 21, no. 3, pp. 934–945, March 2012.
- [27] R. Ferzli and L. J. Karam, "A no-reference objective image sharpness metric based on the notion of just noticeable blur (JNB)," *IEEE Transactions on Image Processing*, vol. 18, no. 4, pp. 717–728, April 2009.
- [28] Z. Wang, H. R. Sheikh, and A. C. Bovik, "No-reference perceptual quality assessment of jpeg compressed images," in *Proc. IEEE International Conference on Image Processing*, vol. 1, 2002, pp. I-477–I-480 vol.1.
- [29] C.-C. Chang and C.-J. Lin, "LIBSVM: A library for support vector machines," *ACM Transactions on Intelligent Systems and Technology*, vol. 2, 2011, Software available at <http://www.csie.ntu.edu.tw/~cjlin/libsvm>.
- [30] K. Seshadrinathan, R. Soundararajan, A. C. Bovik, and L. K. Cormack, "Study of subjective and objective quality assessment of video," *IEEE Transactions on Image Processing*, vol. 19, no. 6, pp. 1427–1441, June 2010.